INFO-GAP ROBUSTNESS FOR THE CORRELATION OF TESTS AND SIMULATIONS OF A NONLINEAR TRANSIENT

François M. Hemez[*]

Engineering Sciences and Applications, ESA-WR

Los Alamos National Laboratory

Mail Stop T006, Los Alamos, New Mexico, U.S.A.

Yakov Ben-Haim[†]

Faculty of Mechanical Engineering

Technion—Israel Institute of Technology

Haifa 32000, Israel

Corresponding author: François M. Hemez

ABSTRACT

An alternative to the theory of probability is applied to the problem of assessing the robustness, to uncertainty in model parameters, of the correlation between measurements and computer simulations. The analysis is based on the theory of information-gap uncertainty, which models the clustering of uncertain events in families of nested sets instead of assuming a probability structure. The system investigated is the propagation of a transient impact through a layer of hyper-elastic material. The two sources of non-linearity are (1) the softening of the constitutive law representing the hyper-elastic material and (2) the contact dynamics at the interface between metallic and crushable materials. The robustness of the correlation between test and simulation, to sources of parameter variability, is first studied to identify the parameters of the model that significantly influence the agreement between measurements and predictions. Model updating under non-probabilistic uncertainty is then illustrated, based on two complementary immunity functions: the robustness to uncertainty and the opportunity from uncertainty. Finally an info-gap model is embedded within a probability density function to represent uncertainty in the knowledge of the model's parameters and their correlation structure. Although computationally expensive, it is demonstrated that info-gap reasoning can greatly enhance our understanding of a moderately complex system when the theory of probability cannot be applied due to insufficient information.

1. INTRODUCTION

One central difficulty in identifying the form of a numerical model and experimentally calibrating the values of its parameters is that the identification and calibration results can be ambiguous. Alternative combinations of model forms and parameter values can yield essentially equally good reproduction of test data.

---

[*] Technical staff member, (+1) 505-663-5204 (Voice); (+1) 505-663-5225 (Fax); hemez@lanl.gov (E-mail).
[†] Professor, Yitzhak Moda'i Chair in Technology and Economics, (+972) 4-829-3262 (Voice); (+972) 4-829-5711 (Fax); yakov@technion.ac.il (E-mail).

This ambiguity is sometimes analyzed in terms of analytical or numerical ill-conditioning or instability. This ambiguity is further exacerbated by the fact that not only decision variables are involved, but numerous other unknown or uncertain variables fluctuate beyond the control of the experimenter, and sometimes even without the experimenter's awareness of their presence or relevance. In short ambiguity can occur whenever "variables"—meaning input parameters, models or conceptual forms—can interact to reproduce the data in more than one way.

Uncertainty plays a central role in calibration and ambiguity of identification. Clearly conceptual ambiguity and numerical ambiguity are the result of imprecision or lack of information, both of which also result from uncertainty. Epistemic uncertainty occurs in modeling activities when the laws that govern the evolution of a system are not known with absolute certainty. More specifically, parameter uncertainty originates from the imprecision with which parameters of a model are measured or identified. Uncertainty, rather than being an accident of the scientific method, is its very nature. (Adapted from a quote of Andrea Saltelli [1].)

This paper addresses the problem of refining a numerical model to make it reproduce the test data to a given level of accuracy. To achieve this objective the correct model form and parameter values must be inferred from the test data. In light of the above discussion this implies that uncertainty must be accounted for and that the robustness of the identification to that uncertainty must be established. That is, we address the question: How much uncertainty in unmeasured variables can be tolerated without changing the identification? If the robustness to uncertainty is great, then the ambiguity is of low significance since the unmeasured variables could vary greatly without inducing a different model. On the other hand low robustness implies significantly ambiguous model identification; the chosen model could change substantially due to even small changes in the unmeasured variables.

In structural dynamics where the preferred analysis method is the finite element method, the model identification problem has been studied extensively [2]. The work presented in this paper departs from the state-of-the-art in finite element model updating in two main ways. First non-linear finite element models are developed to represent fast, transient events. Some of the materials involved exhibit a softening behavior and they cannot be represented with a linear constitutive relation. In addition the dynamical phenomenon of interest is high-frequency wave propagation. It occurs in less than one millisecond and cannot be represented using a truncated basis of low-frequency mode shapes.

Second, due to our fragmentary information and incomplete understanding of the processes involved, uncertainty cannot be represented with the theory of probability. Probability theory is often taken for granted even though it can only be rigorously justified when extensive observations are available. For example assume that X is a random variable with realizations -0.19, +0.73, -0.59, +2.18, and -0.14. If enough samples are available, statistics such as the mean and standard deviation can be accurately estimated. If more samples become available, it might even be possible to estimate the probability density function. However if only the five observations in the previous sequence are known, about all that can be said without adding more information that

is **really** available is that X belongs to an interval of unknown size which is centered somewhere in [-0.59; +2.18]. Not being able to rely on probability implies that uncertainty propagation cannot take advantage of efficient sampling techniques. Therefore the computational cost of the method proposed here for uncertainty propagation should not come as a surprise.

2. UNCERTAINTY AND ITS EFFECT ON COMMON MODELING ACTIVITIES

We start by discussing the effect of uncertainty on common modeling activities such as correlating tests and simulations, and calibrating parameters of a model. The discussion also introduces definitions and notations used throughout this paper.

2.1 Representing Systems and Uncertainties

The numerical model we seek to develop using the finite element method is simply denoted:

$$y = M(q) \tag{1}$$

The model provides a non-linear mapping between y, the output features (such as peak stress, peak acceleration, fundamental resonant frequency), and q, the model's decision parameters (such as the constitutive law, shell thickness, friction coefficient). The selection of q entails both the identification of the model's parameter values as well as the choice between conceptually distinct classes of models. The decision parameters q are distinct from system design decisions or operational decisions based on the model, which are not considered in this paper, which concentrates on the modeling process. A model specified by q is validated when it can be asserted with confidence that q accurately represents the physical properties of the system throughout the design domain or operational space.

In addition to the decision variables q we deal with uncertain variables u represented by an information-gap model (IGM) denoted by $U(u_0;\alpha)$:

$$y = M(q;u), \quad u \in U\big(u_0;\alpha\big) \tag{2}$$

where the IGM will be defined in section 3. The unknown u may represent a damping mechanism that we are not aware of; a coefficient of strain-rate dependency; a non-linear stiffness parameter, etc. We may have information about the uncertain variables u, however this information may be quite fragmentary. We may not even know the identity of some of these uncertain variables. Or we may be unsure whether a given variable should be categorized as a decision variable q or an uncertain variable u. This expresses the fact that the actual sources of uncertainty and their influence on the performance indicators y are incompletely known.

2.2 Robustness: Immunity to Uncertainty

The conventional paradigm for correlation between test measurements and mathematical analysis states that the decision variables q can be chosen to provide a model that reproduces the experimental data with high

fidelity. However due to the ambiguity of identification, different models might perform equally well. One model may be better than the others but we cannot know which.

Furthermore even if a single choice of the decision variables q reproduces the data with higher fidelity than all competing models, we still cannot have confidence that this model is physically valid throughout the design domain. The reason is that the uncertain variables u interact with the decision variables q and thereby preserve the potential for identification ambiguity. The quality of calibration may be due not to the physical validity of q, but to felicitous interaction between q and u.

However when a model is obtained which is true to the data and also highly insensitive to variations of the uncertain variables, then the validity of this model is strengthened. By establishing the ***immunity*** of the decision variables q to the uncertain variables u, we weaken the interaction between the latter and the former and thereby reduce the ambiguity of the identification. This "factoring out" of the uncertain variables strengthens the confidence in the validity of the model throughout the design domain.

3. INFORMATION-GAP MODELING OF UNCERTAINTY

How to factor out the uncertain variables without relying on the theory of probability is the focus of this section. Info-gap models of uncertainty are briefly introduced. A formulation is then proposed to investigate the robustness of test-analysis correlation to sources of uncertainty.

3.1 Test-analysis Correlation

As explained previously, a numerical model is calibrated if it accurately reproduces the test data. The discrepancy between test data y^{Test} and model predictions y can be assessed with different metrics denoted by $R(q;u)$. For instance a mean-squared error metric may be defined:

$$R(q;u) = \frac{1}{N} \sum_{k=1...N} \left(y_k^{Test} - y_k(u) \right)^2 \tag{3}$$

The index k runs over all the repetitions of all the various different tested quantities. Note that predictions y of the model depend upon the decision variables q as well as upon the choice of uncertain variables u. Whatever measure of discrepancy is employed, let R_C denote the greatest level of infidelity that is acceptable. That is, a model is said to be calibrated if:

$$R(q;u) \le R_C \tag{4}$$

A model is "good enough" or "acceptable" if it satisfies equation (4). In other words R_C specifies the level of ***satisficing*** for the model calibration [3]. While the fidelity function $R(q;u)$ depends upon the uncertain or unknown quantities u, it will turn out that this is not an impediment to the analysis. On the contrary it is the

prime mover of the info-gap robustness analysis to be discussed below. The uncertainty of variables u is modeled by an IGM $U(u_0;\alpha)$ which is a family of nested sets parameterized by an uncertainty parameter $\alpha>0$ [3].

3.2 Information-gap Modeling of Uncertainty

Before proceeding with a robustness analysis it is useful to briefly explain how the info-gap models of uncertainty are constructed. An IGM is simply a collection of nested sets of uncertain events. The "size" of these sets is controlled by the horizon-of-uncertainty parameter α. The sets, denoted $U(u_0;\alpha)$, are nested so that $\alpha<\alpha'$ means that $U(u_0;\alpha)$ is included in $U(u_0;\alpha')$. In other words the range of uncertain events increases as the uncertainty parameter α increases. For example describing the random variable X of section 1 with an IGM could consist of establishing nested intervals within which X varies around a nominal value denoted by X_o:

$$U(X_o;\alpha) = \left\{ X \mid |X - X_o| \le \alpha \right\}, \quad \alpha \ge 0 \tag{5}$$

Equation (5) shows that the range of values that the variable X can assume increases without bound as the uncertainty parameter α increases.

Other examples of info-gap models of uncertainty are provided in sections 6, 7, 8 and reference [3]. The key point is that info-gap theory hypothesizes the **structure** of the uncertainty space and expresses how uncertain events cluster around one another, but no measure functions are posited. It is important to realize that an IGM requires less information than is needed for specifying the frequency of occurrence of events in terms of a probability density function. An IGM includes all representations of the uncertain event—that is, all probability distributions, membership or belief functions, intervals, random sets, etc.—that are consistent with the model's structure and horizon-of-uncertainty α.

3.3 Robustness to Uncertainty

The value of the performance level R_C is not chosen a priori. As in all info-gap analyses, the performance level R_C is embroiled in a basic trade-off and its value is chosen in light of the resolution of that trade-off. The basic decision function of info-gap decision theory is the robustness function $\hat{\alpha}$. The robustness of decision q is the greatest value of the uncertainty parameter α at which the model fidelity is never worse than R_C. The robustness is formally defined as:

$$\hat{\alpha}(q;R_C) = \max\left\{ \alpha \ge 0, \text{ such that } \max_{u \in U(u_0;\alpha)} R(q;u) \le R_C \right\} \tag{6}$$

where α is the horizon-of-uncertainty and u_0 denotes the nominal setting of the unknown quantities u.

The significance of the robustness function is that it assesses the degree of variation of the uncertain u that does not jeopardize the fidelity of the model to the data. If the robustness of decision q is large, then the model fidelity is immune to large variations of the unknown quantities u. If $\hat{\alpha}$ is small, on the other hand, then even

very small fluctuations of the uncertain quantities u endanger the model fidelity. The identification of the model is therefore ambiguous when the robustness is small. At low robustness decisions based on the model are likely to be questionable due to the influence of variability and modeling error. Methods for judging whether $\hat{\alpha}$ is 'small' or 'large' are discussed elsewhere [3, chap. 4].

A value of decision variables q whose robustness is large represents a model from which the effect of uncertainty u has been substantially removed. If $\hat{\alpha}$ is large, then we have reason to believe that q represents physically meaningful properties of the system, uninfluenced by the unknown auxiliary terms u.

Note also that the robustness $\hat{\alpha}$ depends on the demanded model fidelity R_C. In fact there is an irrevocable trade-off: the stricter the demanded fidelity (expressed as a small value of R_C), the lower the robustness (manifested in a small value of $\hat{\alpha}$) [4]. Good performance is obtained at the expense of eroded immunity to failure. Examining this trade-off of performance against immunity-to-failure lets the analyst choose an acceptable and feasible level of demanded fidelity R_C. These aspects of decision-making under uncertainty are illustrated in section 7.

4. SHOCK PROPAGATION THROUGH A HYPER-ELASTIC MATERIAL

In this section we describe the experimental system which is studied in this paper. In section 5 we discuss a standard approach for developing a finite element model of such a system, and we discuss the info-gap critique of this standard analysis. In section 6 we formulate and perform the info-gap robustness and opportunity analysis of this system. The analysis is limited to a single uncertain variable, all other uncertain variables being held fixed at their nominal values. The analysis in section 6 is repeated for each of the four uncertain variables. In section 7 we remove the 1-variable constraint, and perform the robustness and opportunity analyses with uncertainty in four variables simultaneously. We discuss implications of the info-gap analysis for system modeling, emphasizing the trade-offs between robustness, opportunity, and fidelity to data.

The application of interest is a high-frequency shock performed in the summer of 1999 at Los Alamos National Laboratory. The experiment was designed to study the propagation of a shock wave through a non-linear, visco-elastic material [5].

4.1 Impact Test Setup

The test consists of dropping from various heights a carriage (drop table) on which are mounted a layer of hyper-elastic material and a steel cylinder. Upon impact on a concrete floor a shock wave is generated that propagates through the hyper-elastic material. The heavy steel cylinder compresses the hyper-elastic pad and causes elastic and plastic strains during a few milliseconds. A photograph of the setup is shown in figure 1-a.

LA-UR-02-3538. **Unclassified**.
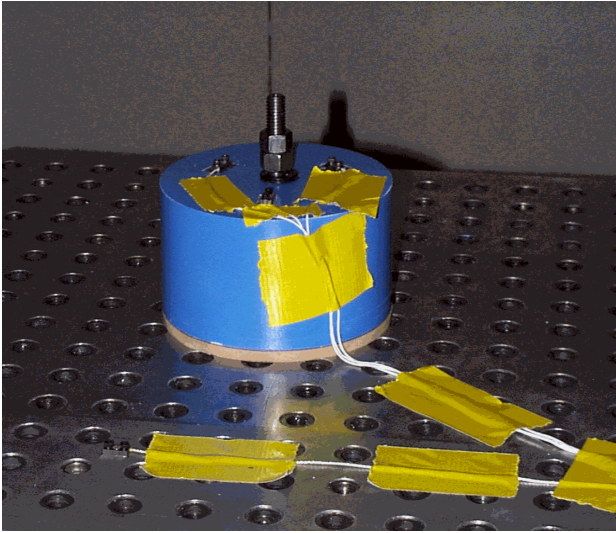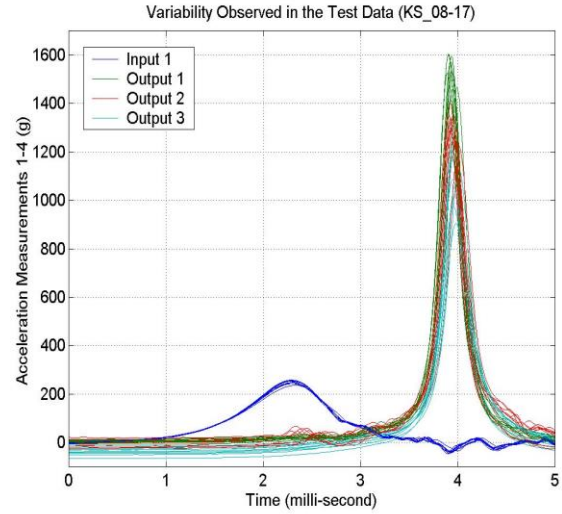
(a) Experimental set-up.   *(b) Signals measured during 10 replicate tests.*

Figure 1: Experimental set-up and acceleration measurements.

Four acceleration measurements were collected during each test. One signal was measured on the top surface of the carriage and the other three were measured on top of the steel cylinder. The former is referred to as the "input" acceleration signal and the latter are the "output" acceleration signals at sensors 1, 2, and 3. Figure 1-b shows the input and output signals obtained when the same test was repeated ten times.
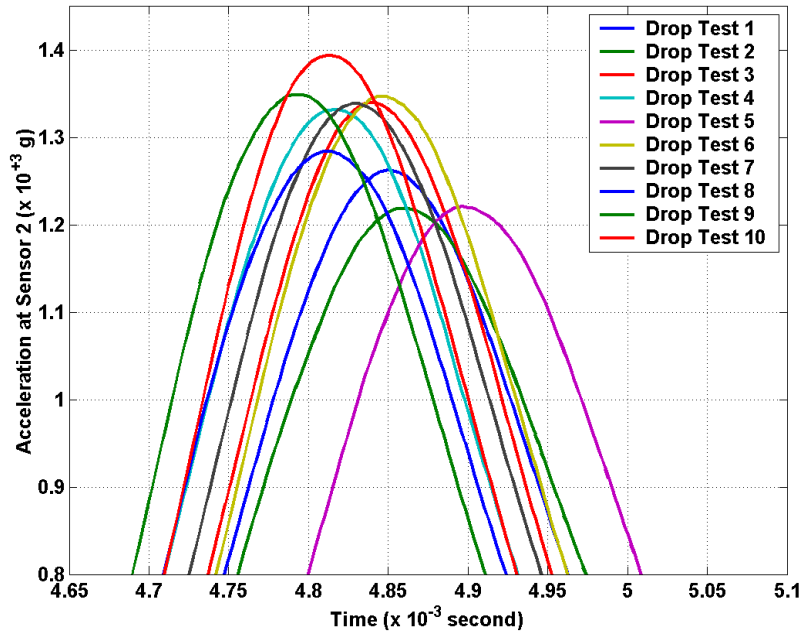

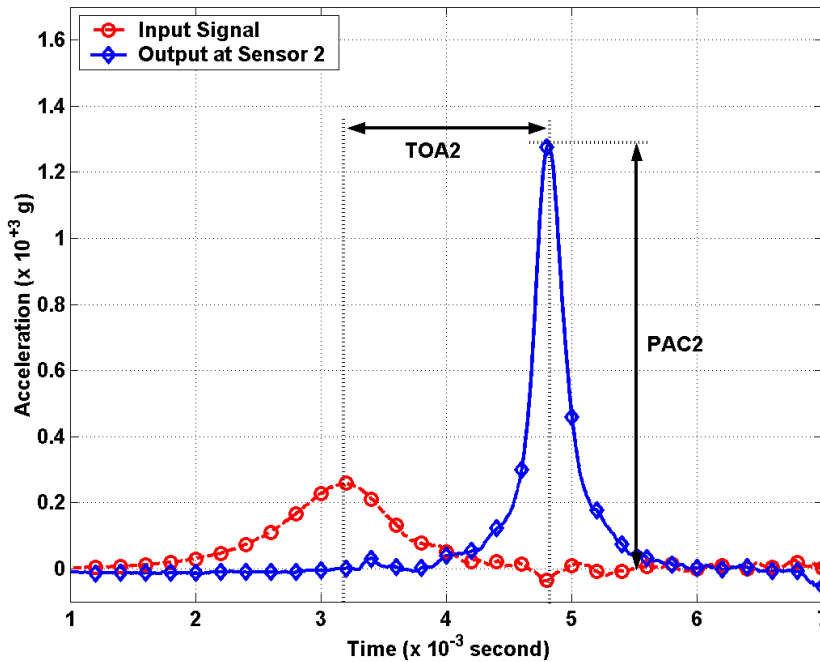*Figure 2: Peak acceleration variability measured at sensor 2.*

Figure 3: Definition of the PAC2 and TOA2 response features.

4.2 Observed Variability and Feature Definition

The reason for replicate testing was to estimate the total variability of the experiment. Because the sources of environmental and operational variability were a priori unknown, the tests were repeated to estimate the total experimental uncertainty. Such uncertainty manifests itself through the variables denoted by *u* in the previous discussion. Figure 2 illustrates the variability of output signals collected at sensor 2 when a 6.3 mm-thick hyper-foam pad is tested and the carriage is dropped from an initial height of 0.33 meters. Overall it can be observed that peak acceleration values vary by 14%. Although not large, ignoring this variability would result in predictions erroneous by several hundred g's, which might suffice to yield catastrophic failure of the system.

To analyze the results of this experiment we focus on the peak acceleration and time-of-arrival at sensor 2. The impulse is so short in time—and the shape of the pulse can be reproduced by a half-sine wave—that matching these two features is sufficient to capture the energy content of the response. In the following, these features of the measured data are denoted by the acronyms PAC2 and TOA2, respectively.

Figure 3 defines the two response features graphically. It is emphasized that the time-of-arrival is not defined as the absolute time at which the signal peaks, but rather as the time it takes the shock wave to travel from the input sensor (located on top of the drop table) to the output sensor (located on top of the steel cylinder).

LA-UR-02-3538. **Unclassified**.

5. FINITE ELEMENT MODELING AND TEST-ANALYSIS CORRELATION

This section describes the finite element simulation developed in response to testing and for the purpose of prediction. The model-building exercise includes an assessment of the sources of uncertainty (section 5.1), and test-analysis correlation that establishes the fidelity of the model (section 5.2). The adequacy of parametric calibration is discussed in section 5.3.

5.1 Finite Element Modeling

Figure 4 illustrates the finite element model developed for numerical simulation. The analysis program used is HKS/Abaqus®-Explicit, a general-purpose package for finite element modeling of non-linear structural dynamics [6]. It features an explicit time integration algorithm, which is convenient when dealing with non-linear material behavior, contact dynamics, and high frequency excitation. The model shown in figure 4 defines 963 nodes, 544 volume elements, and two contact pairs located at the cylinder/pad interface and the pad/carriage interface. It yields a total of 2,889 degrees of freedom composed of structural translations in the three directions and Lagrange multipliers defined for handling the contact constraints. An analysis running on a typical single-processor workstation is executed in approximately 10 minutes of CPU time.

The finite element simulation was parameterized in an effort to capture the material variability, the experimental variability, and other sources of uncertainty. Based on experimental evidence, see figure 1-b, it was decided that the model had to be three-dimensional to represent the fact that the drop table might not always hit the floor perfectly horizontally. Two tilt angles were therefore introduced in the numerical simulation. Another source of variability was the torque applied to the tightening bolts that held the assembly together on the carriage. The applied torque was not measured during testing. A small scaling variation of the measured impulse was also allowed to account for potential sensor calibration errors and other systematic bias introduced by data decimating and filtering. These four parameters are defined in table 1.
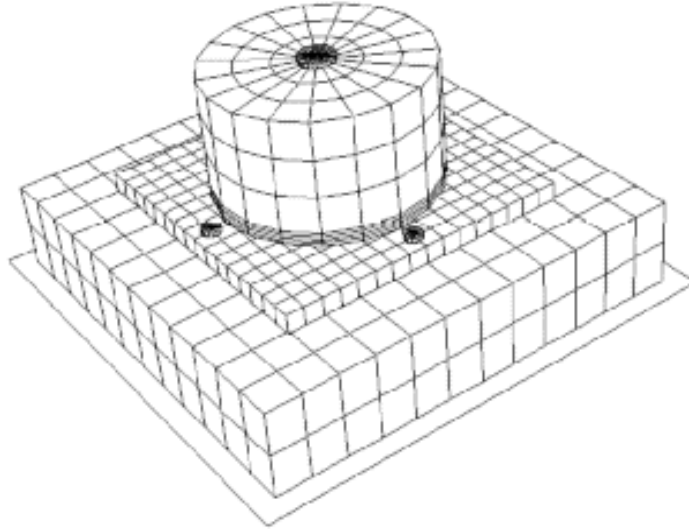
Figure 4: Computational finite element model.

Table 1: Input parameters of the model and their nominal ranges.

Symbol	Definition	Nominal Value	Lower Bound	Upper Bound	Units
θ_1	First tilt angle	0.50	0.00	2.00	Degree
θ_2	Second tilt angle	0.50	0.00	2.00	Degree
P_B	Bolt preload	1.72	0.00	3.45	MPa
s_I	Input scaling	1.00	0.90	1.10	Unitless

Other input parameters are not included in this analysis because previous work has demonstrated that these additional parameters do not explain the observed variability [5, 7]. The tilt angles, bolt preload, and input scaling parameters constitute the decision variables q:

$$q = \{\theta_1 \quad \theta_2 \quad P_B \quad s_I\}^T \tag{7}$$

Typical ranges for the four parameters that control the numerical simulation are shown in table 1. The range of each parameter is established based on experience and physical constraints. For example observation of the carriage's support system suggests that tilt angles greater than one degree are not possible. However it must be stressed that the actual ranges of these variables are not known. The nominal values listed in the table are physically plausible estimates of the parameter values.

5.2 Test-analysis Correlation and Parameter Calibration

We now briefly outline a typical approach to correlate tests and simulations results, and in section 5.3 the limitations of this approach are identified. The info-gap response to these limitations is developed in section 6.

A typical test-analysis correlation study would proceed with a comparison of measured and predicted features to assess the model's accuracy. When the agreement is not deemed sufficient, the input parameters (7) are adjusted to reduce the distance between measurements and predictions. This is illustrated in figure 5, which shows a "2D slice" of the four-dimensional test-analysis metric $R(q)$ defined to assess the distance between measured and predicted features. The metric is defined from the weighted L^2 norm of the prediction error $e(q)$:

$$y(q) = \begin{Bmatrix} \text{PAC2} \\ \text{TOA2} \end{Bmatrix}, \qquad e(q) = y^{Test} - y(q), \qquad R(q) = e(q)^T W_{ee}^{-1} e(q) \qquad (8)$$

where $y(q)$ is the output of the numerical simulation and y^{test} is the vector of average test results. (A variation of this would be to average $R(q)$ over repeated measurements.) The weighting W_{ee} is, here, a constant and diagonal matrix that eliminates the dimensional difference between the units of PAC2 and TOA2. The matrix W_{ee} is the diagonal matrix of observed variances of the measurements of PAC2 and TOA2, whose diagonal elements are [3.4645E+03, 9.6111E-10].
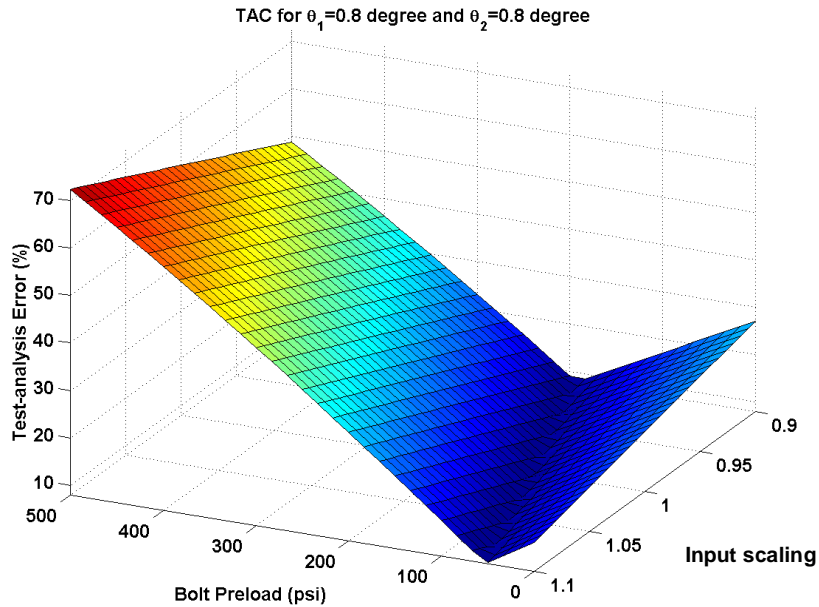
Figure 5: Test-analysis metric R(q) versus parameters P_B and s_I.

Figure 5 shows that various combinations of the decision variables preload P_B and scaling s_I can provide small prediction errors when the tilt angles are kept constant and equal to 0.8 degrees. The response surface was

*LA-UR-02-3538. **Unclassified**.*

generated by analyzing the finite element model at 256 different combinations of the quadruplet $(\theta_1;\theta_2;P_B;s_I)$. Quadratic polynomials were then best fitted through the 256 features PAC2 and TOA2 to interpolate the surface between the points that had not been analyzed. In a typical optimization framework the shape of the response surface would be unknown, and an optimization solver would be wrapped around the finite element code to solve the problem:

$$q^* = \left\{ q, \text{ such that } R(q^*) = \left[\min_{q \in [q_{min}; q_{max}]} \right] R(q) \right\} \tag{9}$$

Hence the ranges listed in table 1 define the four-dimensional hyper-cube design domain within which parameter calibration is sought. The value of the metric at the optimal parameter set, $R^* = R(q^*)$, is the best possible test-analysis error that can be achieved with the current model.

5.3 Issues That Make The Approach in Section 5.2 Inadequate

The test-analysis framework of section 5.2 breaks down because of the severely ambiguous identification of the preload P_B and impulse-scaling s_I variables. We noted in section 5.2 in connection with figure 5 that a continuous range of values of P_B and s_I provides essentially the same fidelity between measurements and predictions. As discussed in sections 1 and 2.2 this ambiguity is a serious impediment to the future application of the updated model in configurations other than explicit test points.

If we knew a probability density function for the preload and scaling variables, ***then*** we could use any of a number of statistical tools to choose a best estimate of these entities, and thereby remove the ambiguity. The reader is referred to references [8, 9] for a discussion of uncertainty assessment, calibration, and validation. The test-analysis correlation metric $R(q)$ is compatible with common tests in conventional statistics [10] or Bayesian statistics [11]. ***However*** we know no such probability density function. The tilt angles and bolt preload vary in unknown ways. Measurements are not available that would justify the choice of a particular probability structure. Simply assuming that these parameters are, for instance, uniformly or normally distributed would be pure conjecture because ***evidence*** is not available to support such an assumption. Making assumptions that are not backed up by strong evidence can lead to erroneous decisions with catastrophic consequences; analysts should be careful not to assume more than is ***really*** known[¶].

Because there is no evidence available to justify the choice of a probability distribution to model the uncertainty of the impact experiment, conventional methods for propagating uncertainty, such as statistical

---

[¶] See, for example, a discussion in reference [12] of the toy-problem "Can the value of y be greater than 1.8 when $y=(a+b)^a$ and $0.1<a<1$, $0<b<1$?" Assuming Gaussian probability distributions for parameters a, b and performing a one million-sample Monte Carlo analysis can yield the answer "Never," which is erroneous. Assuming uniform distributions under-predicts the number of occurrences when $y>1.8$. If the value $y=1.8$ were some critical level not to be exceeded, catastrophic failure could occur as a result of assuming more than is really known—which is that parameter a, likewise b, belongs to an interval, $0.1<a<1$. The location within the interval of the most likely value of parameter a cannot be inferred from the above problem statement.

testing, are of limited utility. It is to remedy this deficiency that the info-gap theory of uncertainty is implemented in this study.

6. THE ROBUSTNESS AND OPPORTUNITY ANALYSES

In section 5 we updated the system model by choosing values of the parameters $(\theta_1;\theta_2;P_B;s_I)$. However, these variables are neither observed nor controlled. In fact, there is every reason to believe that they assume widely different values during different runs and under different conditions. In the remainder of this paper we study the modeling implications of unknown variations of these parameters, around the nominal or estimated values obtained in section 5.

The variables $(\theta_1;\theta_2;P_B;s_I)$ were considered controllable decision variables in the context of parametric calibration (section 5). However, we now regard them as unknown and uncontrollable entities whose uncertainty is represented by an IGM. Henceforth we will denote these variables by $u=(\theta_1;\theta_2;P_B;s_I)$ and reserve q for the decision variables. In sections 6 and 7 it is assumed that the only knowledge about the uncertain variables $(\theta_1;\theta_2;P_B;s_I)$ of the finite element simulation—which in fact are info-gap uncertain—is that they belong to intervals of unknown absolute size and known relative size. Typical intervals are listed in table 1. No evidence is available from which a probability structure might be inferred, and the analysts are not willing to make further assumptions.

The first question we would like to answer is: "***How robust is our design objective to the uncertainty in the variables u?***" The goal is to ensure that the predictions of the finite element model provide acceptable correlation with the tests. Clearly "acceptable" is a subjective and somewhat arbitrary notion that depends on the application. For simplicity, the illustration targets an acceptance level of no more than $R_C=20\%$ error. Answering the above question is, in a broad sense, an issue of sensitivity. We wish to estimate the sensitivity of the performance $R(q;u)$ to variations of the uncertain variables u, where q represents various parameters of the model being developed.

To stress the parallel to the discussion of section 3, it is emphasized that the parameters $u=(\theta_1;\theta_2;P_B;s_I)$ are info-gap uncertain variables because the characteristics of their variations are not known with certainty, and cannot be controlled by the analysts. It is also important to recall that the robustness analysis differentiates between decision variables q (controllable parameters that characterize the system-model begin developed) and uncertain variables u (that represent ancillary uncertainties). This would typically be achieved by categorizing each input parameter either as a decision variable q_k (that can be chosen by the analyst) or an uncertain variable u_k (which is not controllable) in an attempt to obtain a design objective function $R(q;u)$.

6.1 Numerical Procedure

LA-UR-02-3538. **Unclassified***.*

A robustness analysis consists of estimating the horizon-of-uncertainty $\hat{\alpha}$ that guarantees acceptable performance as defined in equation (6). For simplicity, the acceptable performance region is denoted by $R \leq R_C$, and the "failure" region is $R > R_C$. Uncertainty is represented using an IGM of uncertainty denoted by $U(u_0;\alpha)$, as outlined in section 3. The computational and decision-making procedures are conceptually illustrated in figures 6-a and 6-b, respectively. Figure 6-a shows that, at each horizon-of-uncertainty α_k, an optimization problem is solved to provide the worst possible performance $R^*(\alpha_k)$ within the info-gap uncertainty set $U(u_0;\alpha_k)$:

$$R^*(\alpha_k) = \max_{u \in U(u_0;\alpha_k)} R(q;u) \tag{10}$$

The sequence of points $\{\alpha_k; R^*(\alpha_k)\}$ that appear in figure 6-a is then used to approximate the continuous performance curve $R^*(\alpha)$ shown in figure 6-b. Information flows in figure 6-a from the vertical axis (α) to the horizontal axis (R^*). Decision-making is illustrated in figure 6-b, and it reverses the flow of information. For the target performance R_C the tolerable horizon-of-uncertainty $\hat{\alpha}$ is obtained by reading the performance curve $R^*(\alpha)$. The shaded area in figure 6-b represents the acceptable operating region.
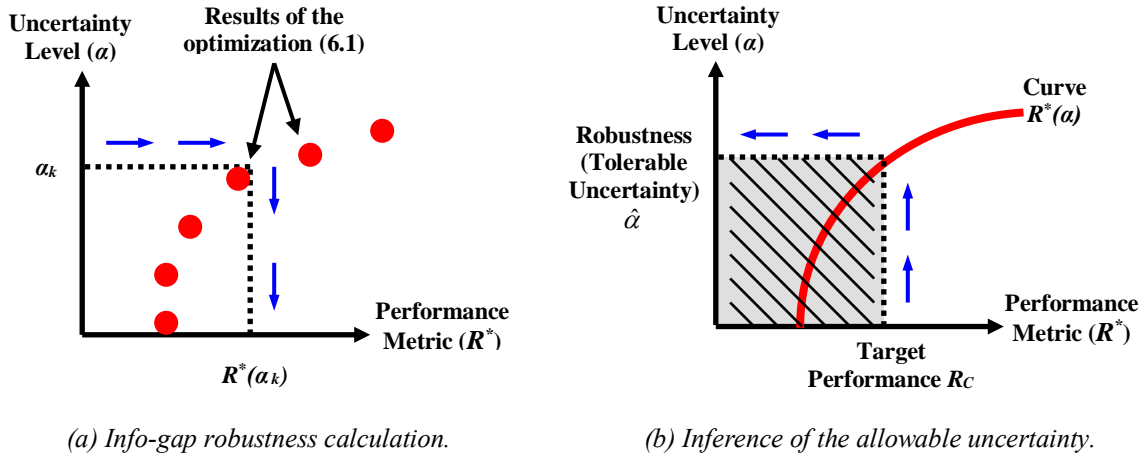

(a) Info-gap robustness calculation.   *(b) Inference of the allowable uncertainty.*

Figure 6: Conceptual illustration of an info-gap robustness analysis.

Of course if the analyst is only interested in estimating $\hat{\alpha}$, it is not necessary to construct the entire curve $R^*(\alpha)$ as illustrated in figure 6. Efficient search strategies can be devised that take advantage of the curve's proven monotonic property [13].

6.2 Robustness Function For Each Variable

The objective of this first analysis is to assess the robustness of test-analysis correlation to parameter uncertainty. Therefore the ***adverse*** aspect of uncertainty is investigated by answering the question: How large can the horizon-of-uncertainty be, without causing unacceptable deterioration of the test-analysis correlation?

The analysis starts in this section with the definition of four info-gap uncertainty levels α_1-α_4, one for each uncertain variable in $u=(\theta_1;\theta_2;P_B;s_I)$. In section 7 we consider the four variables together. The robustness analysis focuses on one uncertain variable u_k at a time, with the other three kept constant and equal to their nominal values. This analysis studies the effect of each input parameter independently from the others. The performance criterion $R(q;u)$ is the test-analysis correlation metric defined in equation (8). The convex domains of uncertainty $U(u_k^0;\alpha_k)$ are simply intervals defined by:

$$U(u_k^0;\alpha_k) = \left\{ u_k \mid \alpha_k u_k^- \leq u_k - u_k^0 \leq \alpha_k u_k^+ \right\} \quad \alpha_k > 0 \qquad (11)$$

where the lower and upper limits u_k^- and u_k^+ represent the minimum and maximum bounds that the parameter u_k cannot exceed. The symbol u_k denotes one of the four unknowns $(\theta_1;\theta_2;P_B;s_I)$, and u_k^0 represents a nominal value. Table 1 defines the nominal values u_k^0, and the quantities u_k^- and u_k^+ are defined as follows. u_k^- is the lower bound minus the nominal value, while u_k^+ is the upper bound minus the nominal value. Thus u_k^- is negative, u_k^+ is positive, and the uncertainty intervals are asymmetric for the angle parameters. Because the dimensionless horizon-of-uncertainty parameter α_k is in fact not known, we confront here not a single specific interval of variation $U(u_k^0;\alpha_k)$, but rather an unbounded family of nested uncertainty intervals $\{U(u_k^0;\alpha_k), \alpha_k>0\}$.
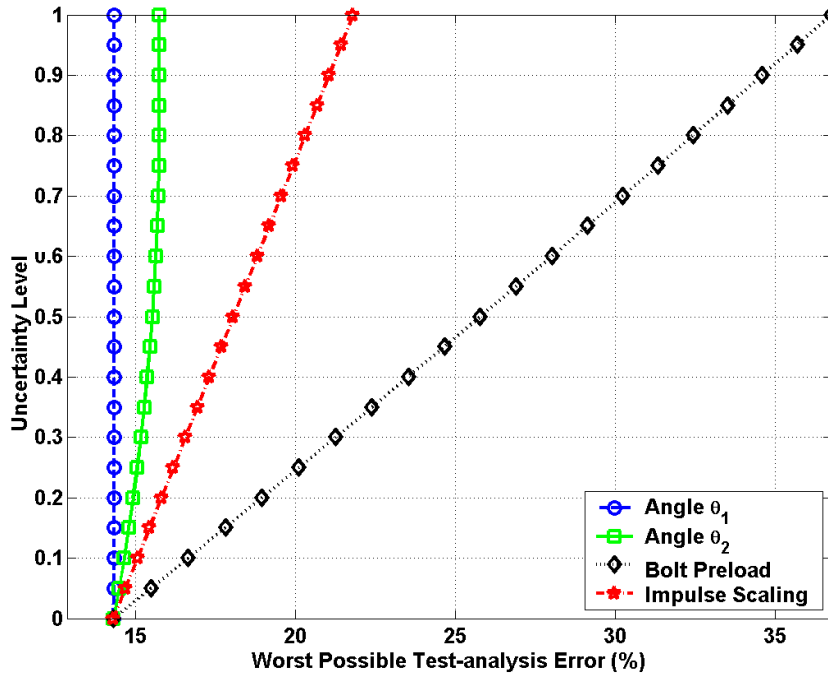

Figure 7: Results of the worst-case info-gap robustness analysis.

Figure 7, which is the realization of the schematic figure 6, investigates the deterioration of the original test-analysis correlation due to uncertainty. The vertical axis is the uncertainty parameter α_k, and the horizontal

axis is the worst quality of model performance, $R^*(\alpha_k)$, defined in equation (10). The optimization searches for the worst correlation at each uncertainty level. A gradient-based BFGS algorithm is wrapped around the HKS/Abaqus® finite element package through a Matlab™ interface. This implementation is feasible only because the algorithm optimizes one variable at a time and requires a small number of finite element calculations to converge, typically 12 to 15. The reason why the worst test-analysis correlation $R^*(\alpha_k)$ increases when the uncertainty level α_k increases is because $R^*(\alpha_k)$ is the solution of the maximization problem (10). For larger horizon-of-uncertainty parameters α_k the search space $U(u_k^0;\alpha_k)$ becomes more inclusive, and the solution $R^*(\alpha_k)$ can only increase.

It can be observed that the most adverse effects of uncertainty are associated with parameters P_B (bolt preload) and s_I (impulse scaling). Uncertainty in the preload P_B has the potential to increase the original 14.5% test-analysis correlation error (at $\alpha=0$) to more than 37% (at $\alpha=1$). Uncertainty in the tilt angles, on the other hand, produces little deterioration of the correlation. Graphically it can be observed that the model is most robust to a lack-of-knowledge in the tilt angles because the slopes of their robustness functions are the steepest, meaning that large horizon-of-uncertainties can be tolerated with little change of the performance. From this analysis we learn that it may not be critical during an experiment to attempt to control or measure the tilt angles. It is also learned that no more than $\hat{\alpha}=24\%$ uncertainty can be tolerated in the knowledge of the bolt preload P_B to guarantee that the test-analysis correlation error remains less than $R_C=20\%$. Such information is read from the figure as $\hat{\alpha}(0.20)=0.24$.

6.3 Opportunity Function For Each Variable

We now investigate the ***beneficial*** aspect of uncertainty. The question is: Can uncertainty be taken advantage of to improve the test-analysis correlation? Stated differently: Can the model performance be substantially better than the nominal performance, even at a low horizon-of-uncertainty?

This question is not to be confused with the previous analysis of robustness. It is in fact defined in reference [3] as a judgment of ***opportunity***. Robustness searches for the greatest info-gap parameter $\hat{\alpha}$ up to which $R(q;u)$ is necessarily at least as good as (no greater than) the demanded performance level R_C. It results in two embedded maximization problems, as shown in equation (6). Opportunity, on the other hand, is the least info-gap parameter α at which $R(q;u)$ can be, but is not necessarily, as good as R_W. To stress the difference with the robustness function previously denoted by $\hat{\alpha}$, the opportunity is denoted by $\hat{\beta}$:

$$\hat{\beta}(q;R_W) = \min\left\{\alpha \geq 0, \quad \text{such that} \quad \min_{u \in U(u_0;\alpha)} R(q;u) \leq R_W\right\} \tag{12}$$

Note that the opportunity function $\hat{\beta}$ is the dual of the robustness function $\hat{\alpha}$ in the sense that the maxima of equation (6) become minima in equation (12). The threshold R_W is the ***windfall performance*** and it is

generally desirable to choose it much smaller than the critical performance R_C, $R_W<<R_C$. In our application the critical performance is the test-analysis correlation error above which predictions of the model are deemed inappropriate, $R_C=20\%$. The windfall performance R_W defines what would essentially be an excellent model with, say, less than $R_W=1\%$ correlation error between test and analysis.

Figure 8 investigates the beneficial potential of uncertainty. The vertical axis is the horizon-of-uncertainty α, and the horizontal axis is the smallest prediction error that can be attained at this uncertainty level—that is, the result of the inner minimum in equation (12). The optimization searches for the best possible correlation at each uncertainty level, as one uncertain variable varies while the others are fixed at their nominal values. When the four uncertain variables are fixed at their nominal values ($\alpha=0$), the nominal performance error of 14.5% is obtained. With a horizon-of-uncertainty of $\alpha=0.1$ favorable variation of the bolt preload can—but does not necessarily—improve the performance to a prediction error of 12%. A reduction of the error to just 1% is possible—though not guaranteed—at a horizon-of-uncertainty of $\alpha=0.55$.
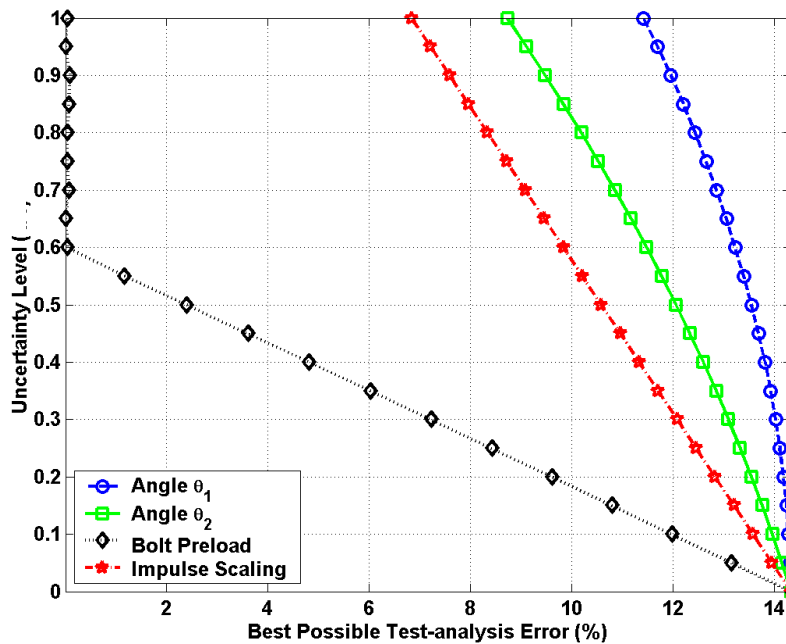

Figure 8: Results of the best-case info-gap opportunity analysis.

As mentioned previously in the case of the robustness analysis, examining the slopes of the opportunity functions is useful in understanding the model sensitivities. Clearly better performance of the model—meaning a smaller test-analysis correlation error—is obtained through a favorable variation of the bolt preload P_B more easily than it can be obtained with the other parameters θ_1, θ_2, or s_I. This can be observed visually by comparing the slopes of the opportunity functions.

From this analysis we learn that the knowledge of the bolt preload P_B is critical to the performance of the model, in terms of both robustness-to-uncertainty and opportunity to reach a better-than-expected test-analysis correlation error. Analysts and experimentalists alike can take advantage of this information to improve their predictive capability and test planning, by indicating the variables to which the predictive accuracy is most sensitive. It is emphasized that the sensitivity analyses presented here differ from conventional sensitivity studies in the sense that (1) sensitivity is not defined through the computation of finite differences, and (2) no probability information is assumed for effect screening or analysis of variance. The analysis here employs only very limited information about the uncertainties which accompany the measurement and modelling process.

7. PERFORMANCE, ROBUSTNESS, AND DECISION-MAKING

After having studied the effect of each uncertainty variable u_k on the performance criterion $R(q;u)$, the robustness and opportunity problems are now solved in the case where the uncertain quadruplet $(\theta_1;\theta_2;P_B;s_I)$ is modeled by a single IGM. The first objective is to identify the allowable amount of uncertainty $\hat{\alpha}$ that provides an acceptable design. The four variables θ_1, θ_2, P_B, and s_I are investigated jointly even though the analysis could be restricted to P_B and s_I because it has been demonstrated in section 6.2 that the prediction error is robust to tilt angle uncertainty. The second objective is to illustrate the cost-benefit analysis that stems from reaching a trade-off between robustness and opportunity.

7.1 Robustness and Opportunity Analyses of the Drop Test Model

According to the procedure described in section 6 the following two optimization problems are solved for values, α_k and β_k, of the horizon-of-uncertainty parameter α:

$$R^*(\alpha_k) = \max_{u \in U(u_0;\alpha_k)} R(q;u), \qquad R_*(\beta_k) = \min_{u \in U(u_0;\beta_k)} R(q;u) \qquad (13)$$

Note that α_k and β_k denote values of the same horizon-of-uncertainty α. Different notations are used to differentiate the robustness function $\hat{\alpha}$ from the opportunity function $\hat{\beta}$. On the left of equation (13), searching for the worst test-analysis correlation error at each uncertainty level provides the robustness function $\hat{\alpha}$. On the right of equation (13), searching for the best test-analysis correlation error provides the opportunity function $\hat{\beta}$. While one always attempts to maximize the robustness-to-uncertainty $\hat{\alpha}$ of a decision, the opportunity $\hat{\beta}$ is minimized because it indicates the least amount of uncertainty that could potentially improve the performance. The robustness and opportunity functions are assessed with respect to $R_C=20\%$ and $R_W=1\%$, respectively.

The uncertainty is represented by a family of nested four-dimensional intervals $\{U(u_0;\alpha), \alpha>0\}$:

*LA-UR-02-3538. **Unclassified**.*

$$U(u_0;\alpha)=\left\{u=\{u_1;u_2;u_3;u_4\}^T \quad \text{such that} \quad -\alpha \le \left(\frac{u_k-u_k^0}{u_k^0}\right)\le\alpha \quad \text{for} \quad k=1...4\right\}, \quad \alpha\ge 0 \tag{14}$$

At any given uncertainty level, $\alpha=\alpha_k$ or $\alpha=\beta_k$, the intervals defined by the IGM (14) provide the constraints for the optimization problems (13). Figure 9 presents the robustness and opportunity functions. It is emphasized that each point in figure 9 is the solution of a four-dimensional optimization problem. Clearly, the info-gap analysis can become demanding in terms of computational resources as the dimension of the IGM increases and more uncertainty levels, $\alpha=\alpha_k$ or $\alpha=\beta_k$, are requested.

The robustness $\hat{\alpha}$ corresponding to an acceptable prediction error of $R_C=20\%$ can be read directly from the curve α-versus-$R^*(\alpha)$ (star symbols, solid line). No more than 17% uncertainty can be tolerated to guarantee 20% test-analysis correlation error. Controlling the uncertainty to no more than 17% during the physical experiments and the development of the numerical model surely comes at a—potentially significant—cost. For example this constraint can be translated into a requirement of the accuracy needed to apply a torque through the tightening of bolts so that the preload does not vary by more than 17% about the measured or estimated value.
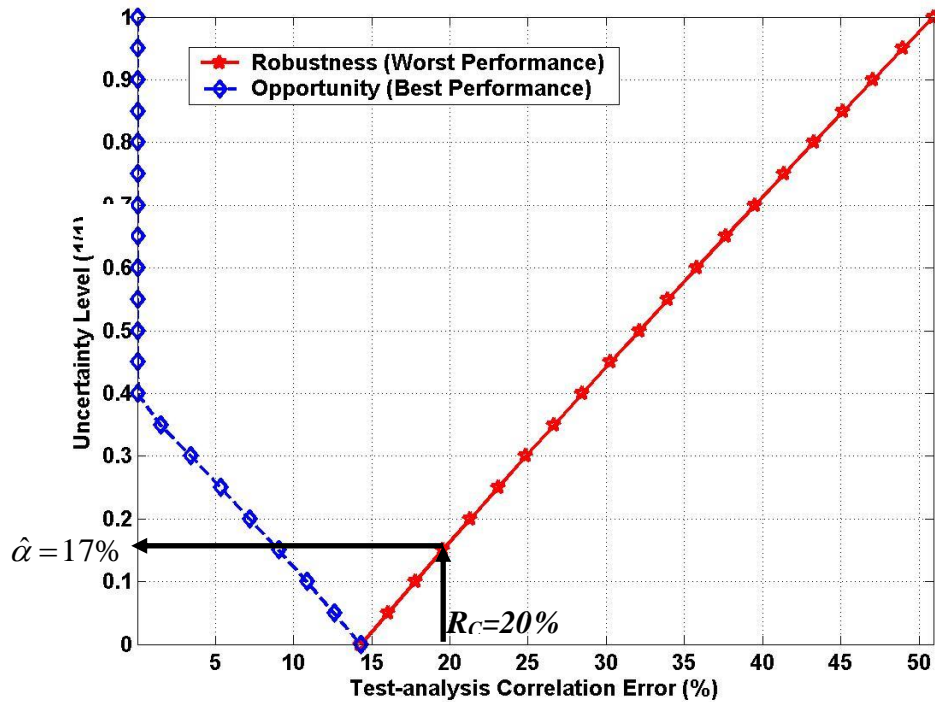

Figure 9: Results of the info-gap robustness and opportunity analyses.

Table 2: Design that provides 1% test-analysis error.

Symbol	Nominal Value	Calibrated Value
θ_1	0.50 degree	0.97 degree
θ_2	0.50 degree	0.98 degree
P_B	1.72 MPa	1.28 MPa
s_I	100.00%	92.52%

The second curve (diamond symbols, dashed line) of figure 9 shows the opportunity function, or the extent to which the modeling uncertainty might result into a better-than-expected performance. As more uncertainty is tolerated, the parameters *(θ_1;θ_2;P_B;s_I)* deviate more from their nominal settings, which enlarges the family of models. At the horizon-of-uncertainty of $\hat{\beta} = 38\%$ the windfall performance of *R_W=1%* error is reached. It means that at least one finite element model gives excellent predictions. The variables *(θ_1;θ_2;P_B;s_I)* that yield less than 1% error between test measurements and model predictions are listed in table 2.

7.2 Accepting Sub-optimal Performance to Enhance Robustness to Uncertainty

The examples we have discussed illustrate that performance—defined, here, in terms of prediction error—can be optimized in the context of non-probabilistic uncertainty. Valuable information is learned about how uncertainty affects performance, without having to rely on probabilistic or approximation methods.

Figure 9 illustrates the important trade-off between sub-optimal performance and robustness-to-uncertainty. The optimum model in the sense of equation (9) is guaranteed to produce no more than 14.5% prediction error. Its robustness to uncertainty, however, is zero. This means that the prediction error can exceed 14.5% as soon as the parameters deviate from the calibrated solution *q**. This makes it difficult to rely with confidence on the predictions of the model in practical situations where some of its parameters are uncertain, as is the case here. Figure 9 also shows that the robustness to uncertainty increases as more prediction error is accepted. If one is willing, for example, to lower the fidelity aspiration from 14.5% error to 20% error, then one can be confident that the predictions will not exceed 20% error even if the parameters of the model deviate up to 17% away from their nominal settings.

The lesson is that model fidelity should not be optimized but rather merely satisfied, which is referred to as *satisficing* in reference [3]. The main benefit is that the decision's robustness-to-uncertainty can be enhanced when the best possible fidelity is not sought. This is important in situations where the model upon which the decision relies is imperfect or not known with absolute certainty.

7.3 Studying the Robustness-opportunity Trade-off for Cost-benefit Analysis

Cost-benefit analysis stems from discussing the trade-off between robustness $\hat{\alpha}$ and opportunity $\hat{\beta}$ functions. Figure 9 shows that, at the 17% uncertainty level, the finite element simulation still provides at least 8% test-analysis correlation error. Obtaining less than 8% error is impossible because $\hat{\beta} = 8\%$ is the result of a minimization problem at the 17% horizon-of-uncertainty. In other words the performance of the model is

20

bounded between 8% and 20% prediction error if the analyst is only willing to accept a 17% lack-of-knowledge with respect to the nominal settings. Contrasting the robustness and opportunity values at a given uncertainty level provides the basic mechanism through which one can estimate the performance enhancement benefits. The other side of the equation is to estimate the cost of not exceeding a specified level of uncertainty or lack-of-knowledge. Reducing the uncertainty typically comes at the cost of performing more tests or implementing higher-fidelity models. Cost assessment is not discussed here because it is purpose-specific and application-dependent to a great extent.

One could, for example, ask what it would take to obtain a finite element model that provides a "near perfect" prediction of the physical test—for instance, less than 1% error. The answer is provided by the opportunity function, $\hat{\beta} = 40\%$. On the other hand a 40% horizon-of-uncertainty only guarantees no more than $R_C=28\%$ test-analysis correlation error. While we seek to obtain a perfect prediction, it could happen that our current model yields some prediction error (up to 28% error). Weighting the cost of controlling no more than 17% uncertainty (with the benefit of guaranteeing no more than $R_C=20\%$ error) against the lesser cost of allowing up to 40% uncertainty (with the risk of deteriorating the test-analysis correlation to 28% error) is the essence of decision-making.

8. HYBRID UNCERTAINTY MODELS FOR TEST-ANALYSIS FIDELITY

Our final application investigates the possibility of combining information-gap models of uncertainty with probabilistic models. The same problem as before is analyzed, that is, the identification of a family of finite element models that provide a given level of prediction accuracy while maximizing the robustness to uncertainty. The main difference is that probability distributions are assumed for random variables (which will be defined). Although no evidence is available to justify this assumption here, the theory of probability is nevertheless utilized to illustrate a situation commonly encountered in engineering applications. It is further assumed that the parameters of the probability distributions are only partially known, and info-gap models are constructed to represent the uncertainty. The example demonstrates one of the many ways in which info-gap uncertainty can be coupled with probability. It also illustrates how several info-gap models can be nested within each other. The problem is formulated in section 8.1 and the info-gap models are introduced in section 8.2. Finally a brief discussion of opportunity versus prediction fidelity concludes the analysis in section 8.3.

8.1 Formulation of the Performance Criterion

As in any info-gap analysis, the formulation starts with the definition of a performance criterion R. The correlation between test measurements and model predictions is assessed through the likelihood of the model given test data. Such a metric is appropriate, for example, in the context of Bayesian inference where the goal is to identify a family of models that best reproduce the available test data, while exploiting a priori information that the analyst has access to about the solution. The unknown variables of the finite element model are, as

LA-UR-02-3538. **Unclassified**.

before, represented by the quadruplet $u=(\theta_1;\theta_2;P_B;s_l)$. Uncertainty in parameters u results in prediction errors $e=y^{Test}-y$ of a model $y=M(q;u)$.

It is assumed that Gaussian probability laws can describe the variations of both parameters u and errors e. We emphasize that such assumption is not, at this point, justified by evidence that might result from empirical observations or expert judgment. It is nevertheless common practice in engineering applications to assume the form of a probability law, if nothing else, to simplify the computational procedure. Using the Bayes rule of posterior probability together with the assumption of Gaussian distributions leads to the well-known formulation of the test-analysis metric R [11]:

$$e(q;u) = y^{Test} - y(q;u), \quad \delta u = u - u_0, \quad R(q;u;v) = \chi^2 = e(q;u)^T W_{ee}^{-1} e(q;u) + \delta u^T W_{vv}^{-1} \delta u \qquad (15)$$

y^{test} is the vector of average test results. (An alternative would be to average $R(q;u;v)$ over repeated measurements.) $y(q;u)$ is the output of the numerical simulation. The matrix W_{ee} is the diagonal matrix of observed variances of the measurements of PAC2 and TOA2, whose diagonal elements are [3.4645E+03, 9.6111E-10].

The performance function (15) follows a Chi-square distribution because the underlying probability laws of u and e are assumed Gaussian. The weighting matrices W_{ee} and W_{vv} are multivariate covariance matrices that must be defined next. First the covariance matrix W_{ee} of the output features PAC2 and TOA2 is estimated from ten replicate experiments and kept constant for the remainder of the analysis:

$$W_{ee} = \begin{bmatrix} 3.46 \times 10^{+3} & -1.34 \times 10^{-3} \\ -1.34 \times 10^{-3} & 9.61 \times 10^{-10} \end{bmatrix} \qquad (16)$$

The second covariance matrix W_{vv} characterizes the variability of the unknown parameters u and it is assumed to possess five independent variance and covariance coefficients v_1-v_5 such that:

$$W_{vv} = E\left[(u-u_0)(u-u_0)^T\right] = \begin{bmatrix} v_1 & v_5 & 0 & 0 \\ v_5 & v_2 & 0 & 0 \\ 0 & 0 & v_3 & 0 \\ 0 & 0 & 0 & v_4 \end{bmatrix} \qquad (17)$$

The preferred scientific method to estimate the coefficients of matrix W_{vv} would be to measure the random variables u in replicate experiments. However we have seen that the parameters u cannot be measured directly. The covariance structure shown in equation (17) results from the judgment that the four variables θ_1, θ_2, P_B, and

s_I are uncorrelated with the exception, possibly, of the two tilt angles[#]. Table 3 defines the nominal variance and covariance coefficients and their assumed ranges.

Table 3: Ranges of the probability law's hyper-parameters.

Symbol	Definition	Design Domain	Nominal Value
v_1	Variance of θ_1	0–15.0 x 10^{-3} degree^2	0.0 degree^2
v_2	Variance of θ_2	0–15.0 x 10^{-3} degree^2	0.0 degree^2
v_3	Variance of P_B	0–5,160.0 x 10^{-3} Mpa^2	0.0 MPa^2
v_4	Variance of s_I	0–16.5 x 10^{-3}	0.0
v_5	Covariance $Cov(\theta_1;\theta_2)$	0–15.0 x 10^{-3} degree^2	0.0 degree^2

The original problem of assessing the test-analysis fidelity of a family of models given four unknown variables u is therefore augmented with the five coefficients of variance denoted by v. A conventional calibration would seek to optimize u such that the prediction error R is minimized. At the optimum an estimation of the posterior covariance matrix (a first-order approximation) would then be calculated as [11]:

$$W_{vv}^{(posterior)} = \left(\left(W_{vv}^{(prior)} \right)^{-1} + \left(\frac{\partial e(u^*;v^*)}{\partial v} \right)^T W_{ee}^{-1} \left(\frac{\partial e(u^*;v^*)}{\partial v} \right) \right)^{-1} \tag{18}$$

Instead of seeking an optimal solution at the expense of sacrificing its robustness to the uncertainty (see section 7.2), the relationship between sub-optimal fidelity, robustness-to-uncertainty, and opportunity-from uncertainty is studied.

8.2 Definition of the Information-gap Models

Uncertainty arises from the unknown calibration variables u and the coefficients of variance v. This situation illustrates the common case where a probability law is assumed whose parameters are unknown. Instead of assuming yet another probability law for the unknown parameters, an IGM is used to represent the parameter uncertainty. The lack-of-knowledge about parameters u and coefficients v is represented by two info-gap models denoted by $U(u_0;\alpha)$ and $V(v_0;\beta)$, respectively.

The first IGM $U(u_0;\alpha)$ describes how the unknown parameters u vary away from their nominal settings u_0 as the horizon-of-uncertainty parameter α increases. Likewise the second IGM $V(v_0;\beta)$ represents the deviation of the variance and covariance coefficients v away from their nominal settings in table 3:

[#] The reason for this choice is that there is no physical reason why the parameters P_B and s_I should be correlated with each other and the tilt angles. Errors in the estimation of the preload P_B are not related to calibration errors represented by s_I. The carriage's support system, on the other hand, might introduce a correlation between the tilt angles θ_1 and θ_2.

LA-UR-02-3538. **Unclassified.**

$$U(u_0;\alpha_u) = \left\{ u = \{u_1;u_2;u_3;u_4\}^T \ \Big| \ -\alpha_u \leq \left(\frac{u_k - u_k^0}{u_k^0}\right) \leq \alpha_u \quad \text{for} \quad k = 1...4 \right\}, \quad \alpha_u \geq 0$$

$$\tag{19}$$

$$V(v_0;\alpha_v) = \left\{ v = \{v_1;v_2;v_3;v_4;v_5\}^T \ \Big| \ 0 \leq \left(\frac{v_k - v_k^0}{v_k^0}\right) \leq \alpha_v \quad \text{for} \quad k = 1...5 \right\}, \quad \alpha_v \geq 0$$

The horizon-of-uncertainty parameters α_u and α_v represent the extent to which the variables u and v deviate from their nominal settings u_0 and v_0, respectively. Note that there is initially no correlation between the tilt angles θ_1 and θ_2, as indicated by $v_5^0 = 0$ in table 3. By allowing the covariance coefficient v_5 to become non-zero the info-gap analysis not only performs a parametric variation of the model's parameters, but it also changes the structure of the model. In the remainder the notation $U(u_0;\alpha_u)xV(v_0;\alpha_v)$ defines the combined info-gap models of uncertainty.

8.3 Discussion of Test-analysis Fidelity and Opportunity From Uncertainty

Once the performance criterion $R(q;u;v)$ and the info-gap models $U(u_0;\alpha_u)$ and $V(v_0;\alpha_v)$ have been established, the numerical implementation is similar to the one presented in section 6.1. Here the discussion is restricted to the opportunity to windfall: How far away from the nominal knowledge $(u_0;v_0)$ should one operate the model to possibly obtain—but not guarantee—performance as good as R_W? What motivates this question is the need to know if the current family of models contains at least one member capable of providing the aspired windfall performance R_W. The model's functional form would typically be questioned if such a model cannot be found, or more physical tests would be requested to better quantify the uncertainty. The answer requires the calculation of the opportunity function.

The main difference with the opportunity analysis reported in section 6.3 and equation (12) is that the Cartesian product of two info-gap models is now used, instead of a single IGM as before. For each performance aspiration R_W an info-gap analysis is performed to identify the opportunity values $(\hat{\beta}_u;\hat{\beta}_v)$ where $\hat{\beta}_u$ and $\hat{\beta}_v$ refer to the opportunity functions associated to the unknown parameters u and v, respectively:

$$\hat{\beta}_u(\hat{\beta}_v;R_W) = \min\left\{ \alpha_u \geq 0 \ \text{such that} \ \hat{\beta}_v = \min\left\{ \alpha_v \geq 0 \ \text{such that} \ \min_{(u;v) \in U(u_0;\alpha_u)xV(v_0;\alpha_v)} R(q;u;v) \leq R_W \right\} \right\} \tag{20}$$

Figure 10 illustrates the performance criterion $R(q;u;v)$ as a function of the opportunity functions $\hat{\beta}_u$ and $\hat{\beta}_v$ labeled "design uncertainty" and "covariance uncertainty", respectively. Each point on the surface represents the result of the optimization of variables $(u;v)$ in a specific domain $U(u_0;\alpha_u)xV(v_0;\alpha_v)$. Convergence is generally reached with about 20 finite element analyses because the number of unknowns is small (four variables u plus five coefficients of variance v).
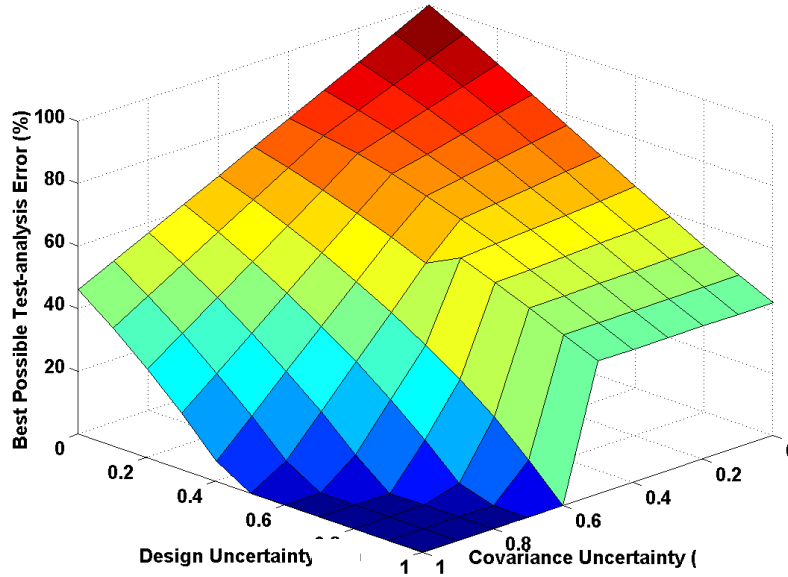
*LA-UR-02-3538. **Unclassified**.*

Figure 10: Opportunity function of the hybrid uncertainty model.

It can be observed in figure 10 that parameter variability and covariance structure uncertainty exhibit a complex pattern of interaction. With small covariance coefficients ($\hat{\beta}_v \leq 50\%$) the best possible test-analysis fidelity is governed by the variables *u*. As the covariance coefficients become more pronounced ($\hat{\beta}_v > 50\%$) and the variability of *u* increases, a dramatic change occurs. The interaction between the two sources of uncertainty suddenly yields models capable of excellent predictions ($R_W=1\%$ error). The analysis demonstrates that finite element models can be found that meet the high aspiration for performance of $R_W=1\%$ test-analysis correlation error. These models are not unique as indicated by the non-trivial shape of the high-fidelity region $\{(\hat{\beta}_u; \hat{\beta}_v) | R(q;u;v) \leq 1\%\}$. The bad news is that such models are located "far away" from the nominal knowledge $(u_0; v_0)$. Figure 10 also provides important information for cost-benefit analysis of the trade-off between experimentation costs with the consequences of ***not*** testing certain regions of the design or operational space.

Table 4: Design that provides 1% test-analysis error.

Symbol	Nominal Value	Calibrated Value
θ_1	0.50 degree	0.99 degree
θ_2	0.50 degree	0.29 degree
P_B	1.72 MPa	2.61 MPa
s_I	100.00%	103.01%

Table 5: Calibrated variance and covariance hyper-parameters.

LA-UR-02-3538. **Unclassified***.*

Submitted to Mechanical Systems and Signal Processing
Hemez78.doc, 13 Nov 2003
Subsequently accepted and published in
2004, vol.18, #6, pp.1443-1467.

Symbol	θ_1	θ_2	P_B	s_I
θ_1	4.8×10^{-3}	1.5×10^{-3}	0	0
θ_2	1.5×10^{-3}	6.7×10^{-3}	0	0
P_B	0	0	$3{,}741.5 \times 10^{-3}$	0
s_I	0	0	0	11.8×10^{-3}

Table 6: Inferred standard deviations and correlation coefficient.

Coefficient	Inferred Value	Percent of Mean
$\sigma(\theta_1)$	0.07 degree	7.0%
$\sigma(\theta_2)$	0.08 degree	28.3%
$\sigma(P_B)$	1.93 MPa	74.1%
$\sigma(s_I)$	0.11	0.1%
Cor Coef($\theta_1;\theta_2$)	0.265	N/A

The values of parameters u and coefficients of variance v that lead to one of the high-fidelity models (that is, $R(q;u;v) \leq 1\%$) are listed in tables 4 and 5, respectively. The resulting standard deviations of parameters $(\theta_1;\theta_2;P_B;s_I)$ and the correlation coefficient between tilt angles θ_1 and θ_2 are given in table 6[**]. Because it was assumed that the unknown parameters u vary according to a multivariate normal distribution, the mean vector and covariance matrix given in tables 4 and 5 suffice to fully specify the probability law. The inference of a probability law whose functional form is unknown can be handled much the same way although it would require wrapping the info-gap analysis around a sampling algorithm to propagate the uncertainty from model inputs to output predictions.

Although the correlation between the tilt angles is relatively small at 0.265, it seems important to obtain a good correlation between measurements and predictions. Comparing the calibration results listed in table 2 (from a pure info-gap analysis) and table 4 (from a probabilistic/info-gap analysis) shows that the values of the first angle θ_1 and input magnitude scaling s_I are consistent. This is confirmed by the less-than-10% standard deviations for θ_1 and s_I shown in table 6. Significant standard deviations, on the other hand, are obtained for the second angle θ_2 and bolt preload P_B. The values of θ_2 and P_B listed in table 4 are less consistent with those listed in table 2, which may be another indication that these parameters vary more than θ_1 and s_I. Valuable information is hence learned that could be used, for example, to perform a probabilistic-based reliability analysis or focus the instrumentation on the parameter P_B that exhibits the most variability during subsequent physical tests.

[**] The standard deviations listed in table 6 are equal to the square roots of variances shown on the main diagonal of table 5. The correlation coefficient between angles θ_1 and θ_2 in table 6 is the covariance divided by the product of the standard deviations from table 5.

LA-UR-02-3538. **Unclassified**.

9. CONCLUSION

The quantification and propagation of uncertainty through a linear model has been the subject of extensive studies in many sciences, especially in the context of probability theory. The relationship between uncertainty and non-linear dynamics is not well understood, the main reason being the difficulty in analyzing non-linear systems. This paper illustrates how information-gap models can be defined and analyzed for studying the propagation of uncertainty through a non-linear finite element simulation without relying on probabilities. The non-linear system considered is the propagation of a transient impact through a layer of hyper-elastic material. The sources of non-linearity are the softening of the constitutive law of the hyper-elastic material and contact dynamics at the interface between metallic and crushable materials.

We have concentrated on establishing the robustness-to-uncertainty of a numerical model in reproducing experimental measurements of a non-linear system subject to a mechanical shock loading. This work demonstrates that model updating under uncertainty can be formulated and solved without relying on the theory of probability. Analysts are therefore offered a practical alternative for situations where only sparse data are available or only limited testing is possible. The main limitation of the approach remains its computational burden, resulting from the need for a sequence of numerical optimizations used for assessing the effect of uncertainty on performance.

Future work will focus on the application of info-gap theory to decision-making and model validation. Model validation—the assessment of a model's predictive accuracy throughout a substantial region of a design domain or operational space—requires correlation with test data. In the case of complex engineering systems it is doubtful that enough validation experiments can be performed to enable statistical tests of validity. Information-gap methods of validation are therefore envisioned as, likely, the only currently available alternative.

10. REFERENCES

[1]   Saltelli, A., Chan, K., Scott, E.M., **Sensitivity Analysis**, *Wiley Series in Probability and Statistics*, Wiley and Sons, West Sussex, England, 2000.

[2]   Mottershead, J.E., Friswell, M.I., "Model Updating in Structural Dynamics: A Survey," *Journal of Sound and Vibration*, Vol. 162, No. 2, 1993, pp. 347-375.

[3]   Ben-Haim, Y., **Information-Gap Decision Theory: Decisions Under Severe Uncertainty**, Academic Press, 2001.

[4]   Ben-Haim, Y., "Robust Rationality and Decisions Under Severe Uncertainty," *Journal of the Franklin Institute*, Vol. 337, 2000, pp. 171-199.

[5]   Schultze, J.F., Hemez, F.M., Doebling, S.W., Sohn, H., "Statistical Based Non-linear Model Updating Using Feature Extraction," *19th SEM International Modal Analysis Conference,* Kissimmee, FL, Feb. 5-8, 2001, pp. 18-26.

[6] **Abaqus™/Explicit**, User's Manual, Version 6.2, Hibbitt, Karlsson & Sorensen, Pawtucket, RI, 2001.

[7] Hemez, F.M., Wilson, A.C., Doebling, S.W., "Design of Computer Experiments for Improving an Impact Test Simulation," *19th SEM International Modal Analysis Conference,* Kissimmee, FL, Feb. 5-8, 2001, pp. 977-985.

[8] Doebling, S.W., Hemez, F.M., Schultze, J.F., "Validation of the Transient Structural Response of a Threaded Assembly," *4th AIAA Non-deterministic Approaches Forum*, AIAA-2002-1644, Denver, CO, April 22-25, 2002.

[9] Doebling, S.W., "Structural Dynamics Model Validation: Pushing the Envelope," *International Conference on Structural Dynamics Modeling: Test, Analysis, Correlation and Validation*, Madeira Island, Portugal, June 3-5, 2002.

[10] Hemez, F.M., Doebling, S.W., "Inversion of Structural Dynamics Simulations: State-of-the-art and Orientations of the Research," *25th ISMA International Conference on Noise and Vibration Engineering*, Leuven, Belgium, Sept. 13-15, 2000, pp. 403-413.

[11] Hemez, F.M., Doebling, S.W., "A Validation of Bayesian Finite Element Model Updating for Linear Dynamics," *17th SEM International Modal Analysis Conference,* Kissimmee, FL, Feb. 8-11, 1999, pp. 1545-1555.

[12] Oberkampf, W.L., Helton, J.C., Joslyn, C.A., Wojtkiewicz, S.F., Ferson, S., "Challenge Problems: Uncertainty in System Response Given Uncertain Parameters," *Workshop of the Sandia Epistemic Uncertainty Project*, Sandia National Laboratories, Albuquerque, NM, August 6-7, 2002.

[13] Vinot, P. Cogan, S. Ben-Haim, Y., "Reliability of Structural Dynamics Models Based on Info-gap Models," *20th SEM International Modal Analysis Conference,* Los Angeles, CA, Feb. 4-7, 2002, pp. 1057-1063.